PORTLAND
PRESS

## Research Article

# Prematurity negatively affects regenerative properties of human amniotic epithelial cells in the context of lung repair

Dandan Zhu[1,2], Gina D. Kusuma[1,2], Renate Schwab[1,2], Siow Teng Chan[1,2], Jean Tan[1,2], Mohamed I. Saad[1,2], Kristen T. Leeman[3,4], Carla Kim[5], Euan M. Wallace[1,2] and Rebecca Lim[1,2]

[1]The Ritchie Centre, Hudson Institute of Medical Research, Clayton, Victoria 3168, Australia; [2]Department of Obstetrics and Gynaecology, Monash University, Clayton, Victoria 3800, Australia; [3]School of Medicine, The University of Queensland, Brisbane, Queensland, Australia; [4]Division of Newborn Medicine, Department of Paediatrics, Boston Children's Hospital, Harvard Medical School, Boston, MA, U.S.A.; [5]Boston Children's Hospital Boston Stem Cell Program, Department of Genetics, Harvard Medical School and Harvard Stem Cell Institute, MA, U.S.A.

**Correspondence:** Rebecca Lim (Rebecca.lim@hudson.org.au)

OPEN ACCESS

There is a growing appreciation of the role of lung stem/progenitor cells in the development and perpetuation of chronic lung disease including idiopathic pulmonary fibrosis. Human amniotic epithelial cells (hAECs) were previously shown to improve lung architecture in bleomycin-induced lung injury, with the further suggestion that hAECs obtained from term pregnancies possessed superior anti-fibrotic properties compared with their preterm counterparts. In the present study, we aimed to elucidate the differential effects of hAECs from term and preterm pregnancies on lung stem/progenitor cells involved in the repair. Here we showed that term hAECs were better able to activate bronchioalveolar stem cells (BASCs) and type 2 alveolar epithelial cells (AT2s) compared with preterm hAECs following bleomycin challenge. Further, we observed that term hAECs restored *TGIF1* and *TGFβ2* expression levels, while increasing *c-MYC* expression despite an absence of significant changes to Wnt/β-catenin signaling. *In vitro*, term hAECs increased the average size and numbers of BASC and AT2 colonies. The gene expression levels of Wnt ligands were higher in term hAECs, and the expression levels of *BMP4, CCND1* and *CDC42* were only increased in the BASC and AT2 organoids co-cultured with hAECs from term pregnancies but not preterm pregnancies. In conclusion, term hAECs were more efficient at activating the BASC niche compared with preterm hAECs. The impact of gestational age and/or complications leading to preterm delivery should be considered when applying hAECs and other gestational tissue-derived stem and stem-like cells therapeutically.

## Introduction

Idiopathic pulmonary fibrosis (IPF) is characterized by the continual loss of functional lung parenchyma and its replacement by excessive and disordered extracellular matrix, resulting in an eventual decline in respiratory function [1]. The survival rate for IPF is a bleak median rate of 3 years, and it is the most prevalent of the idiopathic interstitial lung diseases [2]. There is increasing evidence indicating that accelerated alveolar senescence is a major underlying factor in the development and perpetuation of IPF [3]. As a chronic disease that affects the aged population (average age of IPF onset is 66 years) [2], it is likely that stem cell attrition contributes to the aberrant wound healing response. Perinatal stem cells such as umbilical cord-, placenta-, amniotic- and chorionic-derived mesenchymal stromal cells are being investigated in clinical [4,5] and preclinical studies [6] as treatment modalities for IPF. However, information around the impact of donor gestational age on the potency of the isolated cells remains scarce. If perinatal stem cells are to be considered as a cell therapy for IPF, it is prudent to understand the impact of prematurity

on cell quality as these differences would inform donor acceptance criteria and key elements in the design of potency assays.

In line with these concepts, we sought to understand the impact of donor gestational age on human amniotic epithelial cells (hAECs) and their ability to activate endogenous lung stem/progenitor cells in the setting of bleomycin-induced lung injury. The alveolar epithelium consists of two main cell types: cuboidal type 2 alveolar epithelial cells (AT2), which secrete high levels of surfactant protein C (SFTPC or SPC), and squamous type 1 alveolar epithelial cells (AT1), which comprise 95% of the gas exchange surface area. The latter express podoplanin (Pdpn) and advanced glycosylation end product-specific receptor (AGER) [7–9]. Genetic lineage-tracing studies have established that AT2 represent lung epithelial progenitors, which proliferate and differentiate during lung maintenance. Following injury, AT2 give rise to AT1 *in vivo*. *In vitro,* AT2 give rise to alveolospheres (alveolar-like structures) that consist of both AT1 and AT2 [10]. Bronchioalveolar stem cells (BASCs) reside at the bronchioalveolar duct junctions (BADJ) of adult lungs and express both SPC and Club cell 10-kDa protein (CC10 or CCSP). The BASCs serve as multipotent lung progenitors capable of differentiating into distal AT1 and AT2, as well as proximal bronchiolar lineages following a lung insult [11,12].

Our previous work showed that hAECs isolated from healthy term placenta, released exosomes that could increase BASC and AT2 numbers and this observation coincided with reduced lung inflammation and fibrosis in bleomycin-challenged mice [13]. And while the hAECs have recently entered the clinical testing phase for chronic lung disease in infants [14] and adults [15,16], it is yet unclear how prematurity of birth might influence the overall efficacy of these cells. We previously reported that hAECs from premature births had greater proliferative potential but reduced anti-fibrotic effects [17]. In our present study, we used the bleomycin-induced lung injury murine model to determine if prematurity of hAEC donors would be associated with changes to their ability to activate BASCs, an endogenous stem/progenitor cell population in the lungs. Specifically, we were interested in the differences in cell signaling pathways that underpin functional differences between term and preterm hAECs. Further, we utilized a three-dimensional (3D) organoid air–liquid interface culture system to determine the direct effects of prematurity on the ability of hAECs to support the growth of lung stem/progenitor cells *in vitro*.

# Materials and methods
## Isolation of human amniotic epithelial cells
Amniotic membranes were collected immediately after cesarean sections from term (37.5 ± 0.5 gestational weeks) and preterm (30.4 ± 3.7 gestational weeks) placentae with 8 placentae included per group. Clinical justifications for preterm delivery included intrauterine growth restriction and preeclampsia. All patients gave written informed consent in accordance to human research ethics guidelines set out by Monash Health. Isolation of hAECs was performed as previously described [18,19]. Access to human tissues was obtained from The Ritchie Centre's Tissue Bank (approved HREC No. 01067B).

## Animals
*In vivo* lung injury was induced in 6- to 8-week-old-female C57BL/6 mice (Monash Animal Services, Victoria, Australia), through intranasal instillation of bleomycin (0.3U each, Bristol Myers Squibb, NY, U.S.A.). After 24 h, mice were administered either 4 million (term or preterm) hAECs suspended in 0.2 ml saline or saline alone via intraperitoneal injection. Animal groups were as follows: (1) control group (saline + saline): saline administered intranasally (vehicle for bleomycin) and intraperitoneally (vehicle for hAECs); (2) saline-treated injured group (bleo + Saline): bleomycin administered intranasally and saline intraperitoneally; (3) injured group treated with term hAECs (bleo + term hAECs): bleomycin administered intranasally and term hAECs intraperitoneally; and (4) injured group treated with preterm hAECs (bleo + preterm hAECs): bleomycin administered intranasally and preterm hAECs intraperitoneally. Group sizes are indicated in each figure legend. Animals were humanely culled 5, 7 or 14 days. The same control group was used for comparison at each time point. All experiments were performed in Monash Medical Centre animal facility and in accordance with the Australian Code of Practice for the Care and Use of Animals for Scientific Purpose with approval from Monash University Animal Ethics Committee (MMCA2010/34).

## Immunofluorescence (IF) staining of lung tissues
Following euthanasia, lungs were perfused with saline and then inflated with 4% (w/v) paraformaldehyde (PFA) at a pressure of 12 cm $H_2O$ and fixed for 24 h prior to paraffin embedding. De-paraffinized lung sections (5 μm) were incubated in 1 mg/ml sodium tetrahydroborate (Sigma, Burlington, U.S.A.) in phosphate-buffered saline (PBS) to minimize aldehyde-induced non-specific autofluorescence background. Citrate antigen retrieval was performed

prior to blocking in 5% goat serum (Thermo Fisher Scientific, Waltham, U.S.A.). Tissue sections were then incubated overnight with rabbit anti-pro-SPC (1:300, AB3786, MilliporeSigma, Burlington, U.S.A.) and goat anti-CC10 (1:200, SC-9772, Santa Cruz Biotechnology, Dallas, U.S.A.). The slides were then incubated with anti-rabbit 568 (1:200, A10042, Life Technologies, Carlsbad, U.S.A.) and anti-goat 488 (1:200, A21467, Life Technologies, Carlsbad, U.S.A.) at room temperature for 1 h. Nuclear staining was performed using 1 mM 4′,6-diamidino-2-phenylindole (DAPI, 1:5000, MilliporeSigma, Burlington, U.S.A.).

Quantification was performed by a blinded observer as follows: at least 18 terminal bronchioles and 6–10 fields of view of alveolar epithelium from 5 to 8 mice per each group were scored staining for pro-SPC, CC10, β-catenin and DAPI. Fluorescence microscopy and imaging were performed with Nikon C1 Inverted Microscope and NIS-Elements software. The average numbers of BASCs per terminal bronchiole were determined by manual counting while the percentage of AT2 cells and the percentage of positive β-catenin staining were determined using Imaris software (Bitplane, Zurich, Switzerland).

## Culture of bronchioalveolar stem cell and AT2 organoids

The establishment of 3D BASC and AT2 organoids was performed as previously described [20]. Briefly, freshly isolated BASCs or AT2s ($2 \times 10^3$ cells per well) were mixed with Matrigel containing MECs ($2 \times 10^4$ cells per well) and cultured in triplicate on transwell inserts (6.5 mm, pore size 5.0 μm). At D3, term or preterm hAECs ($2 \times 10^5$ cells per well) were added to the media in the lower chamber of transwells ($n=4$). After 14 days in culture, imaging was performed at 100× magnification (Leica AF6000LX, Leica Microsystems, Wetzlar, Germany). Numbers, sizes and phenotypes (i.e., alveolar, bronchiolar and bronchioalveolar) of organoids were counted and measured. The phenotypes of organoids were also confirmed by immunofluorescence staining as previously described [21]. Organoids were sized and enumerated using ImageJ. Organoids were randomly allocated to gene expression analysis and immunofluorescence staining. Organoids of each phenotype were dissociated and subjected to RNA isolation.

## Quantitative polymerase chain reaction (PCR)

Total RNA was extracted using the RNeasy Mini Kit or Micro Kit (Qiagen, Limburg, Netherlands), and cDNA synthesis was performed using the SuperScript III Kit (Invitrogen, Carlsbad, U.S.A.). The RT-qPCR was performed using the Fluidigm Biomark™ HD system according to manufacturer instructions. All gene expression studies were performed using Taqman Assays (Applied Biosystems, Foster City, U.S.A.). Human Taqman probe sets were used for hAECs and mouse Taqman probe sets used for organoids and mouse tissues. Targeted genes and their assay IDs are listed in Supplementary Table S1. Relative gene expression was determined using the $2^{-\Delta\Delta Ct}$ method and normalized against GAPDH. MicroRNA expressions profiles for term and preterm hAECs (pooled term or preterm hAECs from five cell lines each) were determined using the Taqman OpenArray Human Advanced miRNA Assays. The miRNA expression was normalized against U6 and analysis performed using Diana Tools-mirPath v.3.

## Statistical analysis

Statistical analysis was performed using GraphPad Prism statistics software (GraphPad Software Inc, San Diego, CA, U.S.A.). All data were presented as mean ± SD. A one-way analysis of variance (ANOVA) was carried out to compare the mean values of different study groups. Unpaired *T*-test was carried out to compare the mean values between term and preterm hAECs in culture experiments. Differences were considered significant at $P<0.05$.

# Results
## Term hAECs induced activation of BASCs and AT2 following bleomycin challenge

Low engraftment rates of hAECs led us to postulate that their beneficial effects may be associated with an activation of endogenous stem/progenitor cells in the lungs [22,23]. We were also interested in the impact of hAEC administration on BASCs and AT2s given their involvement in alveolar epithelial repair [24], particularly in the context of bleomycin-induced lung injury, where hAEC administration has been previously shown to be protective [25,26].

Identification of BASCs at the terminal bronchioles was performed by immunohistochemical staining for pro-SPC and CC10 (Figure 1A). The average number of BASCs per terminal bronchiole is indicative of the activation status of the niche [10,19]. At D5, no significant changes were observed in the average numbers of BASCs at terminal bronchioles between groups (Figure 1B). At D7, BASC numbers were increased in both saline-treated injured group and term hAEC-treated group compared with the control group, but this increase was only significant in the term hAEC-treated group (Figure 1B, $P<0.0001$). By D14, the number of BASCs in term hAEC-treated mice returned to
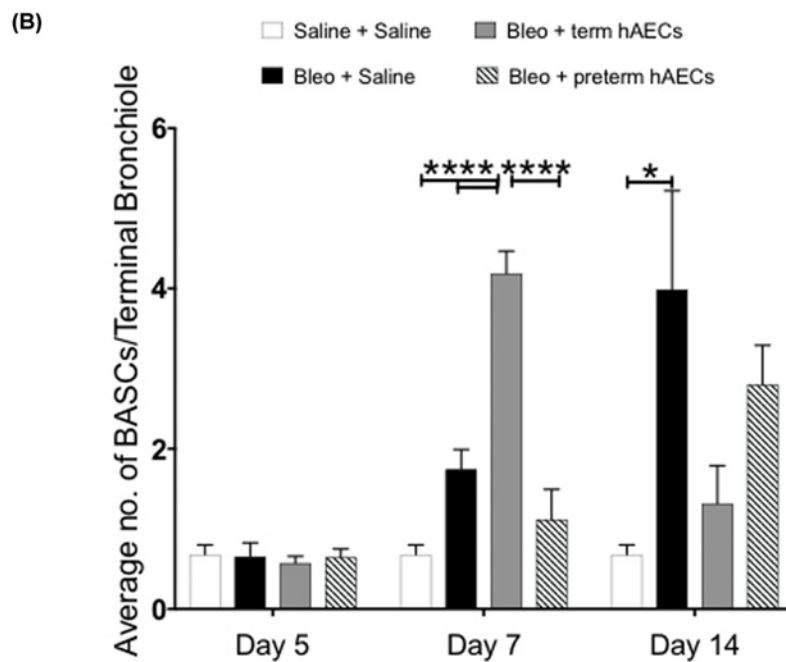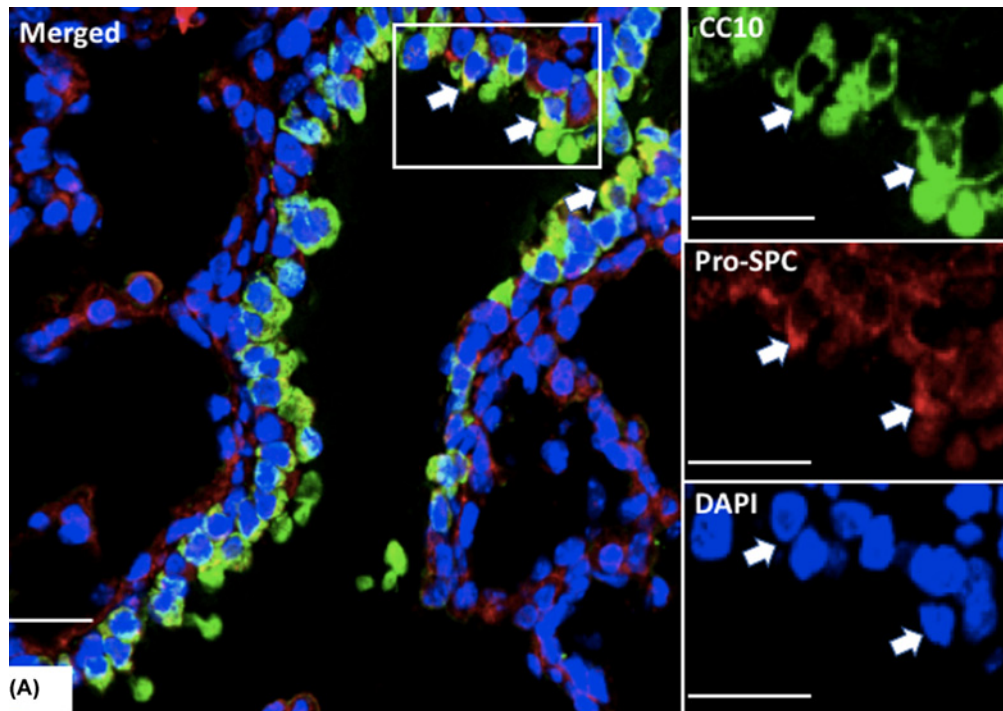
**Figure 1. Immunofluorescence of bronchioalveolar stem cells (BASCs) in mouse lung tissue at D5, D7 and D14 (n=6)**
(**A**) Representative images of BASC immunofluorescence staining; scale bar = 20 $\mu$m. BASCs are located in the terminal bronchioles and are positive for both pro-surfactant protein C (pro-SPC) and Club Cell 10 kD protein (CC10). (**B**) The number of BASCs was significantly increased in the term hAEC treated group at D7 and returned to the level comparable with the healthy controls at D14. However, no significant changes of BASC number were observed in the preterm hAEC-treated group across all the time points. Statistical significance was determined with one-way ANOVA accompanied by the Bonferroni post-hoc test. (*$P$<0.05, ****$P$<0.0001)
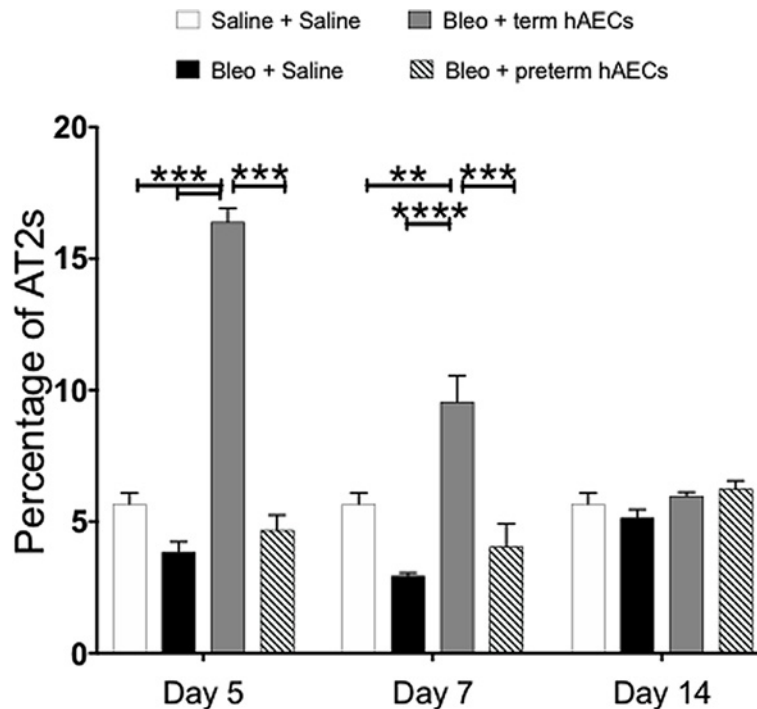
**Figure 2. Percentage of type 2 alveolar epithelial cells (AT2s) in mouse lung tissue at D5, D7 and D14 ( *n*=5).**
Type 2 alveolar epithelial cells are cells that are positive for pro-surfactant protein C (pro-SPC), but negative for Club Cell 10 kD protein (CC10). At D5, the percentage of AT2 population increased dramatically in the term hAEC treated group, and this change was sustained to D7. By D14, there were no significant differences between groups. Statistical significance was determined with one-way ANOVA accompanied by the Bonferroni post-hoc test (**$P<0.01$, ***$P<0.001$ ****$P<0.0001$).

numbers that were comparable with healthy controls, suggesting that the bronchioalveolar duct junction stem cell niche had returned to a state of quiescence. Unlike BASCs, the percentage of AT2 population increased dramatically in the term hAEC-treated group on D5, ($P<0.0001$ compared with control, Figure 2), and was sustained until D7 ($P=0.0069$, Figure 2). By D14, there were no significant differences between groups (Figure 2).

## Neither term nor preterm hAECs altered activation of β-catenin in lung tissues

The β–catenin-dependent Wnt signaling pathway (Wnt/β-catenin pathway) plays a vital role in stem cell development, maintenance and self-renewal, and the activation of this pathway leads to the transcription of genes that control cell fate, polarity and migration [27]. Given our observations around hAEC administration on BASC/AT2 activation, β-catenin expression in the lung tissues was measured (Figure 3A), but no significant differences in either nuclear staining or total staining were observed at either D7 or D14 (Figure 3B,C). While these findings may initially suggest that Wnt/β-catenin signaling is not the major driver of hAEC initiated endogenous stem/progenitor cell activation, it is plausible that the transient nature of hAECs entrapment in the lungs [20] may have had an equally transient effect on Wnt/β-catenin signaling that abated by D7. Accordingly, we assessed the transcription of genes related to the Wnt/β-catenin pathway in lung tissues on D14. Here we observed that *BMP4, RARRES2, SFRP2, TGFβ2* and *WIF1* gene transcription were decreased in saline-treated bleomycin mice compared with control mice ($P=0.0042$, Figure 4A; $P<0.0001$, Figure 4B; $P=0.0011$, Figure 4C; $P=0.0096$, Figure 4D; $P=0.0003$, Figure 4E). The gene transcription of *TGIF1* in term hAEC treatment groups was comparable with control but remained higher compared to saline and preterm hAEC treated groups ($P=0.0129$ and $P=0.0207$, respectively, Figure 4F). There was no difference in *MYC* levels between term and preterm hAECs (Figure 4G); however, endogenous *MYC* expression increased following term hAEC treatment ($P=0.0143$ and $P=0.0269$, compared with controls and saline treated injured groups, respectively, Figure 4H).
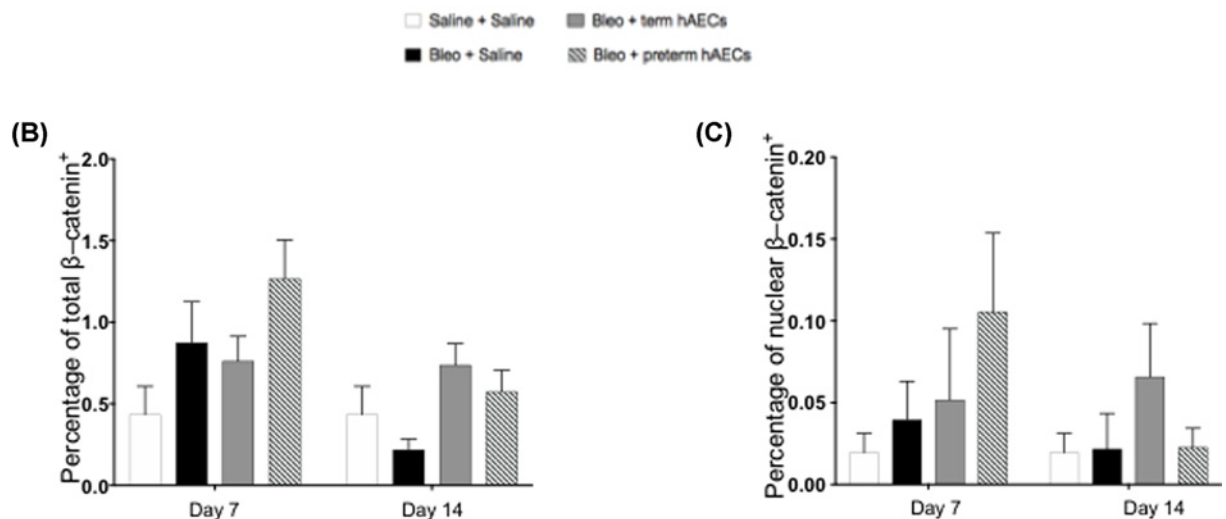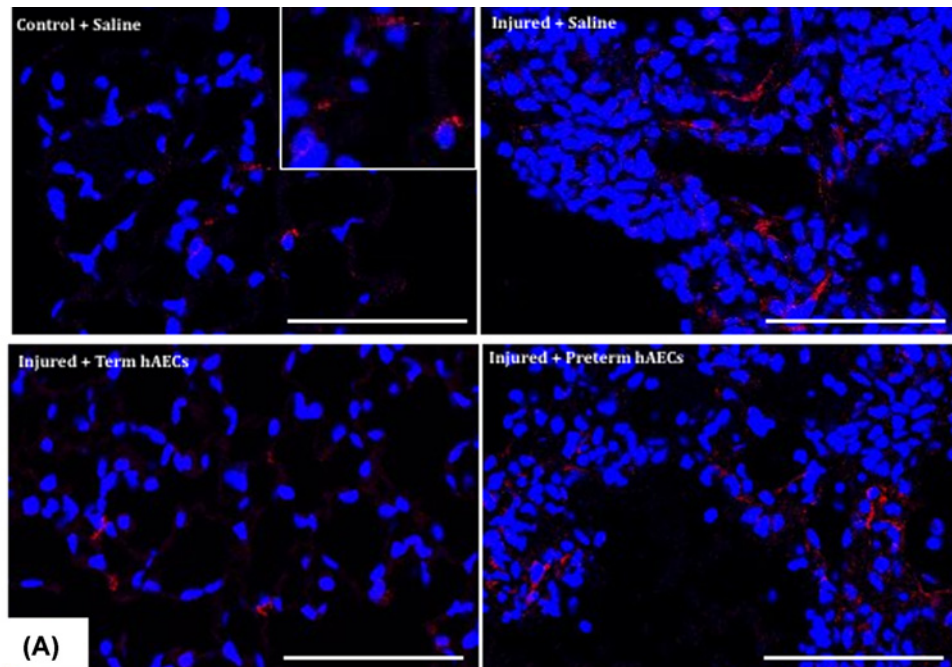
Figure 3. Beta-catenin (β-catenin) immunofluorescence in mouse lung tissue at D7 ( *n*= 6) and D14 (*n*=5).
(**A**) Representative images of β-catenin staining; scale bar = 100 μm. (**B** and **C**) There is no significant differences in the total or nuclear β-catenin expression levels across all the groups on both D7 and D14.

## Term hAECs enhanced organoid-forming efficiency of BASCs and AT2s *in vitro*

Next, we sought to assess if hAECs were able to exert a direct effect on lung progenitor cells. We used an established 3D lung organoid system where BASCs or AT2 were indirectly co-cultured with either term hAECs or preterm hAECs as depicted in Figure 5A. In line with previous reports [20], BASCs can give rise to organoids with three distinct phenotypes: alveolar, bronchiolar and bronchioalveolar, while AT2 cells are only capable of forming alveolar structures (Figure 5B). In keeping with their morphology, alveolar organoids expressed pro-SPC, bronchiolar organoids expressed CC10, and bronchioalveolar organoids were found to express pro-SPC and CC10 (Figure 5C).
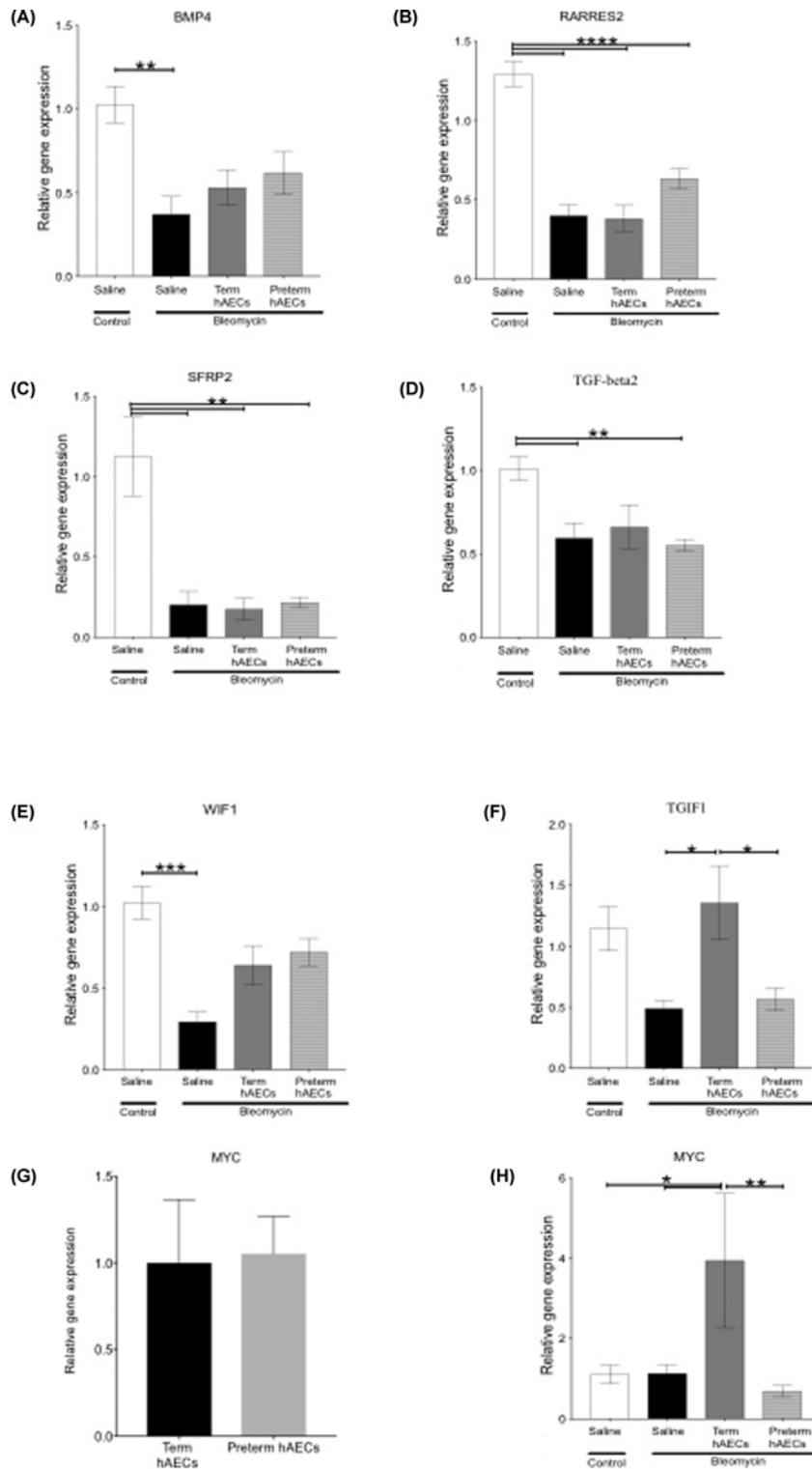
**Figure 4. Changes of Wnt/β-catenin pathway related gene transcription levels in mouse lung tissues on D14 ( *n*=6), and gene transcription level of *MYC* in term/preterm hAECs.**

Transcription levels of *BMP4* (**A**), *RARRES2* (**B**), *SFRP2* (**C**), *TGFβ2* (**D**) and *WIF1* (**E**) were decreased in saline-treated bleomycin mice compared with control mice. Gene transcription of *TGIF1* (**F**) in term hAEC treatment groups was comparable with control level and was remained higher than saline and preterm hAEC-treated groups. There was no difference in *MYC* (**G**) levels between term and preterm hAECs; however, the level of *MYC* (**H**) was increased only in term hAEC treatment groups compared with other groups (*$P < 0.05$, **$P < 0.01$, ***$P < 0.001$, ****$P < 0.0001$).
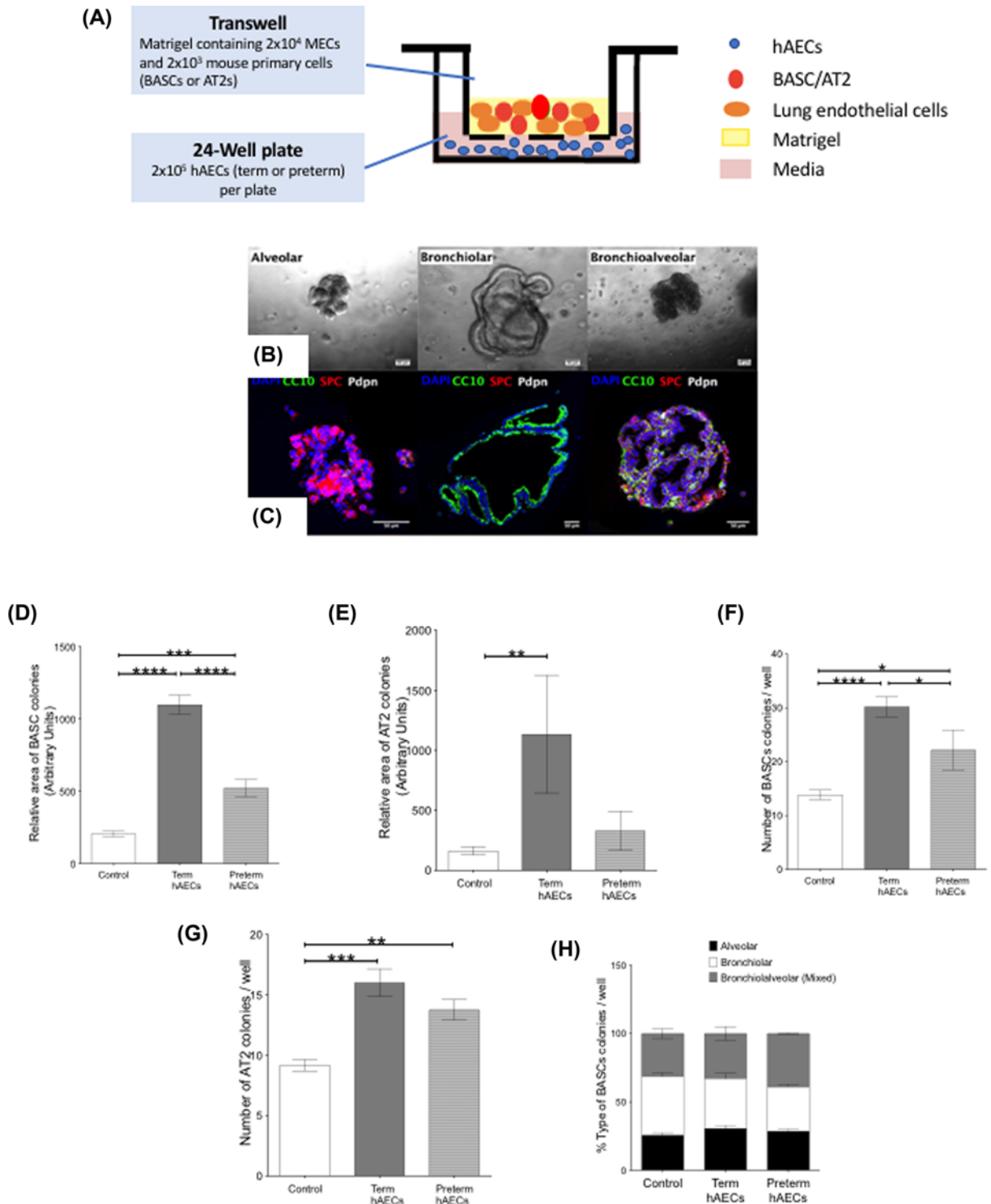
**Figure 5. Bronchioalveolar stem cells and AT2s *in vitro* culture (*n*=4).**
(**A**) Diagram of BASC and AT2 co-culture. (**B**) Representative images of alveolar, bronchiolar and bronchioalveolar organoids after 2 weeks of culture; scale bar = 50 μm. (**C**) Representative images of alveolar, bronchiolar and bronchioalveolar organoid immunofluorescence staining; scale bar = 50 μm. (**D** and **E**) Area of BASC and AT2 colonies. Term hAECs significantly enhanced the size of both BASCs and AT2 *in vitro*, compared with preterm hAECs. (**F** and **G**) Number of BASC and AT2 colonies. Both term and preterm hAECs significantly increased the number of both BASCs and AT2 *in vitro*, and term hAECs increased the number of BASCs compared with preterm hAECs. (**H**) The percentage of each type of colony. There is no difference between groups. Statistical significance was determined with one-way ANOVA accompanied by the Bonferroni post-hoc test (*$P<0.05$, **$P<0.01$, ***$P<0.001$, ****$P<0.0001$).

PORTLAND
PRESS
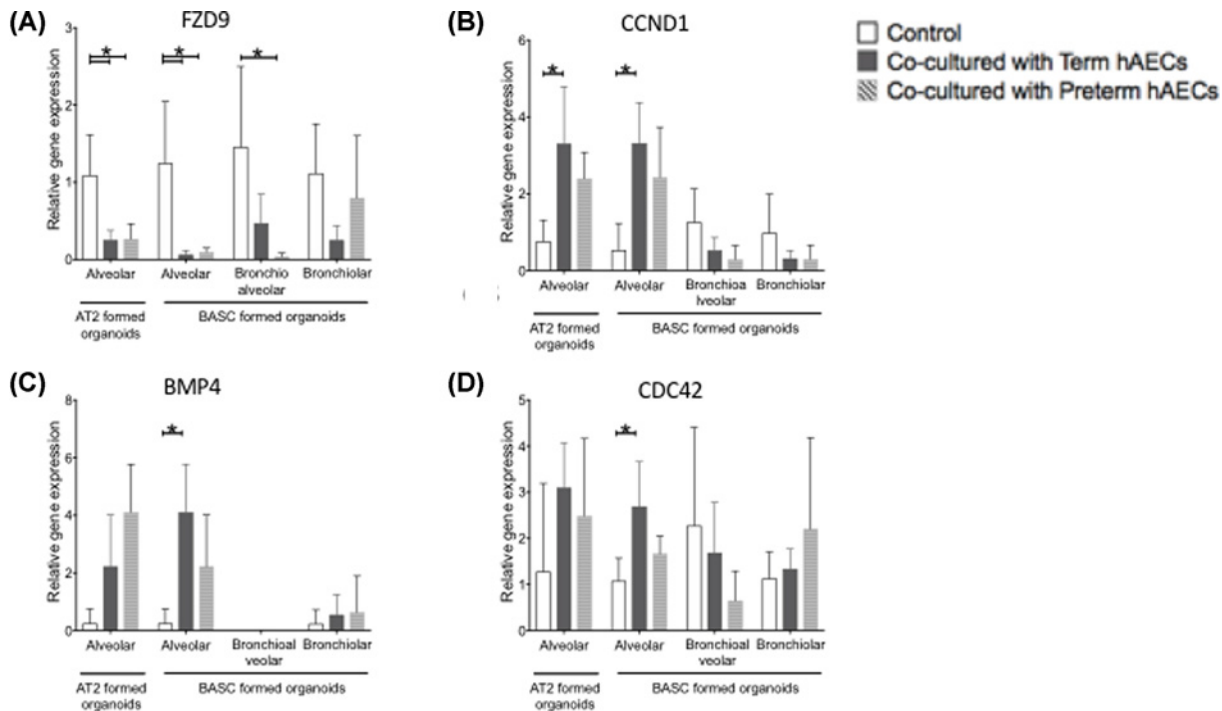


**Figure 6. Changes of Wnt/β-catenin pathway related gene transcription levels in BASC and AT2 organoids ( *n*=4).**
(**A**) Gene transcription of *FZD9* in alveolar organoids was decreased when co-cultured with either term or preterm hAECs. (**B**) Gene transcription of *CCND1* in alveolar organoids was elevated only when co-cultured with term hAECs. (**C** and **D**) Bone morphogenetic protein 4 and *CDC42* transcriptional levels were increased in term hAEC group in BASC formed alveolar organoids (*$P<$0.05).

Our results indicate that term hAECs significantly enhanced the proliferation and organoid-forming efficiency of both BASCs and AT2 *in vitro*, compared with preterm hAECs. This was reflected in the increased sizes of BASC and AT2 organoids formed (Figure 5D,E) as well as the number of BASC organoids formed (Figure 5F,G). However, there was no significant change in the lineage commitment of lung progenitors (Figure 5H).

## Term hAECs increase transcription of Wnt/β-catenin related genes in 3D lung organoids

Given that the expression levels of Wnt/β-catenin signaling target genes were changed in hAEC-treated bleomycin challenged mice, we next examined the expression levels of Wnt/β-catenin pathway related genes in the organoids to determine if this pathway was involved in term hAEC induced BASC and AT2 proliferation. Both term and preterm hAECs reduced gene transcription of *FZD9* in alveolar organoids generated from AT2s ($P$=0.0175 and $P$=0.0194 respectively, Figure 6A), and BASCs ($P$=0.0167 and $P$=0.0196 respectively, Figure 6A). In contrast, only term hAECs increased the gene transcription of *CCND1* in alveolar colonies arising from AT2 and BASCs ($P$=0.017 and $P$=0.0135 respectively, Figure 6B). Furthermore, *BMP4* and *CDC42* transcriptional levels were only increased in alveolar organoids from BASCs co-cultured with term hAECs ($P$=0.0129 and 0.0224 respectively, Figure 6C,D). In BASC-derived bronchioalveolar organoids, *FZD9* transcription was decreased only when co-cultured with preterm hAECs ($P$=0.0357, Figure 6A). There was no change in transcription levels of Wnt/β-catenin related genes in BASC-derived bronchiolar organoids across the groups.

## Term hAECs express higher WNT ligands than preterm hAECs

Having observed differential expression of downstream Wnt targets in the organoids and mouse lung tissues, we next asked if this was attributed to differential expression of Wnt ligands in the term and preterm hAECs. Gene expression analysis revealed that both term and preterm hAECs expressed the Wnt ligands *WNT2, WNT3, WNT5A, WNT6, WNT 7B* and *WNT11* to a similar extent. However, *WNT1, WNT4, WNT10A* and *WNT16* were only expressed in term hAECs not preterm hAECs, and gene expressions levels of *WNT2B, WNT5B, WNT7A* and *WNT10B* were significantly higher in term hAECs compared with preterm hAECs (Figure 7). *WNT3A, WNT8A, WNT8B, WNT9A*
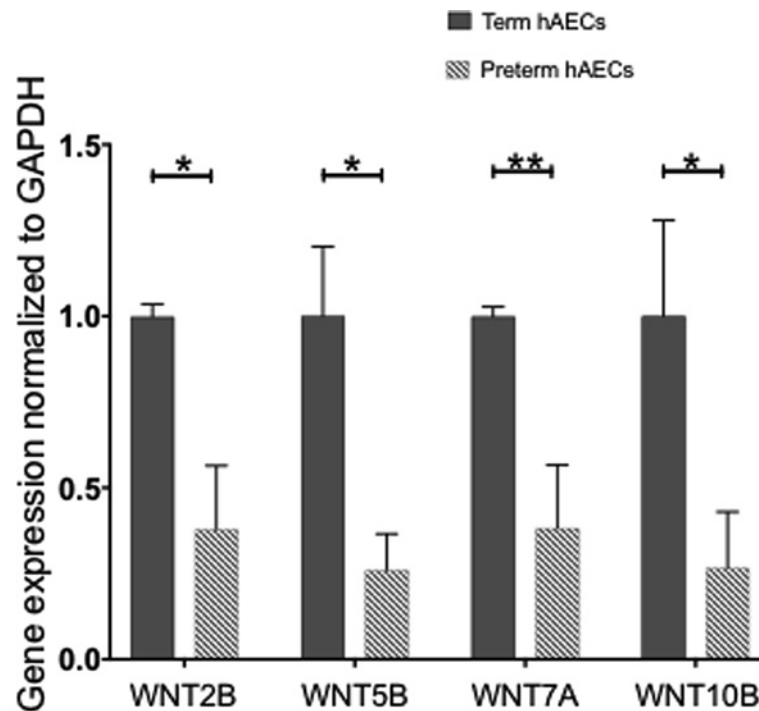
**Figure 7. Changes in Wnt ligand transcription levels in both term and preterm hAECs ( *n*=8).**

Gene expressions levels of *WNT2B, WNT5B, WNT7A* and *WNT10B* were significantly higher in term hAECs compared with preterm hAECs. Statistical significance was determined with one-way ANOVA accompanied by the Bonferroni post-hoc test (*$P$<0.05; **$P$<0.01).

and *WNT9B* were not detected in either term or preterm hAECs.

## miRNAs are differentially expressed between term and preterm hAECs

Comparing miRNA expression between term and preterm hAECs, we observed that 28 miRNAs were only expressed in term hAECs, 40 miRNAs were only expressed in preterm hAECs, and 345 miRNAs were co-expressed in both preterm and term hAECs (Figure 8). Of the co-expressed miRNAs, 101 miRNAs that were expressed at 2-fold or higher (Supplementary Table S2) in term hAECs compared with preterm hAECs. *A posteriori* analysis of pathways union identified the pathways significantly targeted by the most up-regulated 22 miRNAs (expressed 4-fold higher in term hAECs compared with preterm hAECs, Supplementary Table S3). When significantly over-represented pathways were ranked according to the numbers of miRNA targeted, we noted that a number of signaling pathways associated with stem cell development, maintenance and self-renewal were identified. These included the Hippo, p53, TGF-β, regulating pluripotency of stem cells and Wnt signaling pathways.

Of the co-expressed miRNAs, 19 miRNAs that were expressed 2-fold lower (Supplementary Table S4) in term hAECs compared with preterm hAECs. *A posteriori* analysis of pathways union was applied (Supplementary Table S5). We noted that Hippo, p53, TGF-β, regulating pluripotency of stem cells and PI3K-Akt signaling pathways associated with stem cell development, maintenance and self-renewal were identified.

Since Hippo signaling pathway was in both pathways unions with the greatest significance, we also noted that Hippo-related genes *SMAD3*, *SMAD7*, *ID2*, and *YAP1* were associated with up-regulated miRNAs. Connective tissue growth factor (*CTGF*) was associated with downregulated miRNAs, and *LATS1*, *LATS2*, *SMAD2*, *SMAD4*, and *BIRC5* were associated with both up-regulated and down-regulated miRNAs. We proceeded to assess the transcription of these genes and observed that *YAP1* and *LATS1* gene transcription were increased in term hAEC treated bleomycin mice compared with control mice ($P$<0.05, Figure 9A,B), and gene transcription of *BIRC5* were increased in preterm hAEC-treated group compared with control group ($P$<0.05, Figure 9C).
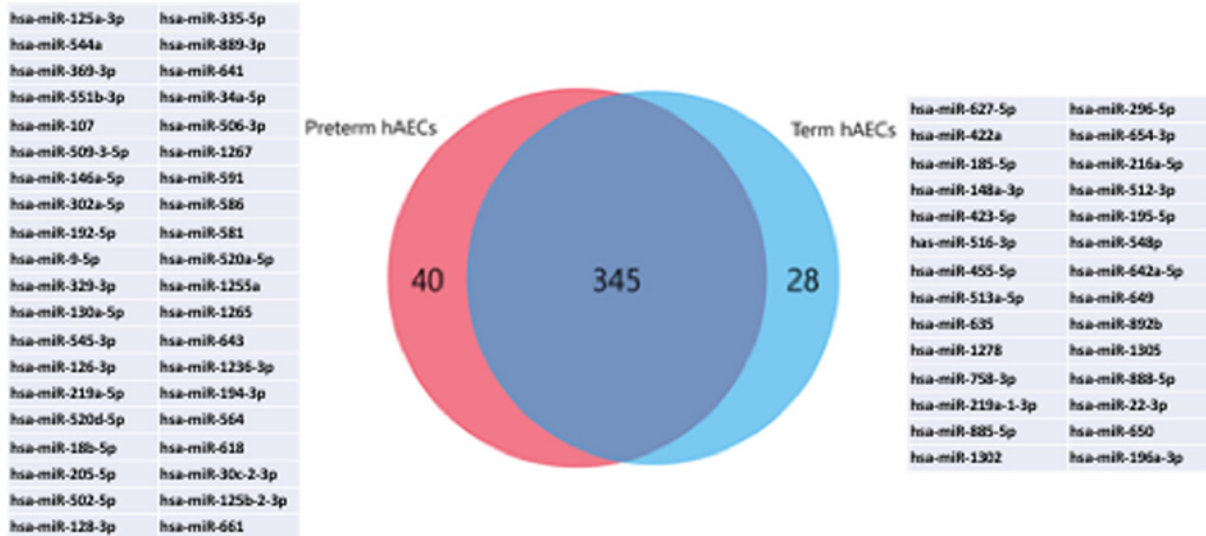
**Figure 8. Venn diagram showing overlap of miRNAs expressed in term and preterm hAECs.**

There were 345 miRNAs co-expressed in both preterm and term hAECs, while 28 miRNAs were only expressed in term hAECs and 40 miRNAs were only expressed in preterm hAECs.
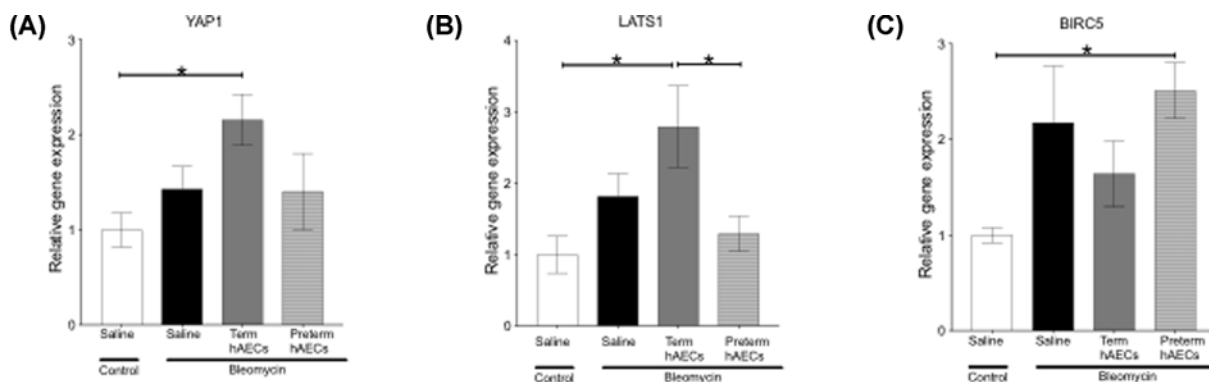


**Figure 9. Changes in Hippo pathway related gene transcription levels in mouse lung tissues on D14 ($n$=6).**

Yes-associated protein 1 (**YAP-1, A**) and *LATS1* (**B**) gene transcription were increased in term hAEC-treated bleomycin mice compared with control mice, and gene transcription of *BIRC5* (**C**) were increased in preterm hAEC-treated group compared with control group. Statistical significance was determined with one-way ANOVA accompanied by the Bonferroni post-hoc test (*$P$<0.05).

# Discussion

The initial discovery of the therapeutic potential of hAECs has moved into the sphere of clinical translation where the safety and tolerability of these allogeneic perinatal stem-like cells are being evaluated across a number of clinical indications. While we and others have shown that hAECs isolated from term, healthy placentae can have potent pro-regenerative potential, there is little information on the impact of prematurity of the donor on the quality of the cells. In the present study, we describe key differences between hAECs obtained from term and preterm pregnancies when applied to a bleomycin model of lung injury, with specific focus on their impact on endogenous lung/progenitor cells. Term hAECs had greater capacity to activate endogenous stem/progenitor cells without significant changes to Wnt/βcatenin signaling. Both term and preterm hAECs mitigated the reduction of *BMP4* and *WIF1* gene expression levels in response to bleomycin challenge. Furthermore, only term hAECs restored *TGIF1* and *TGFβ2* expression levels, while increasing c-*MYC* expression. In an *in vitro* co-culture system, term hAECs increased the average size as well as number of BASC and AT2 colonies without significant changes to lineage commitment. These observations were associated with differential expression of Wnt ligands in the term and preterm hAECs, and Fzd receptors in the BASC and AT2 organoids.

The existence of a BASC population was first described in 2005, as a subpopulation of lung stem/progenitor cells arising from the bronchioalveolar duct junction [11]. They are resistant to bronchiolar and alveolar damage but proliferate during epithelial cell renewal. They are also responsible for maintaining bronchiolar Club cells and alveolar cells in the distal lung [11]. Indeed, recent RNA sequencing of isolated BASCs has shown that they bear a transcriptionally distinct profile that co-expresses bronchiolar and alveolar epithelial genes, and while generally quiescent during homeostasis, the BASC population is the major source for regeneration of distal lung epithelial [28].

In the present study, we observed that BASCs were activated earlier in mice that received term hAECs compared with preterm hAECs. Where injured mice were administered the vehicle (saline), significant BASC activation was seen at D14, this was seen at D7 in mice administered term hAECs. In comparison, mice administered preterm hAECs achieved an attenuated BASC activation response at D14 (Figure 1). Furthermore, we observed significant AT2 expansion only in mice that received term hAECs (D5 and 7, Figure 2). These findings indicate that there are inherent differences between hAECs isolated from term pregnancies compared with preterm pregnancies. Indeed, we had previously reported that hAECs from preterm pregnancies had limited antifibrotic and anti-inflammatory potential [17]. We had proposed in this earlier study that this finding was in large part due to the lower levels of immunomodulatory HLA-G in preterm hAECs [17]. In the present study, we report that term hAECs also have superior ability to activate endogenous stem/progenitor cells in the lungs compared with their preterm counterparts.

In particular, the BASCs and AT2 cells, function as facultative stem cells that can be induced to proliferate and differentiate in response to injury [29]. That term hAECs but not their preterm counterparts were able to induce an early expansion of the BASC population (D7 compared with D14 expansion seen in untreated, spontaneously recovering animals) suggests that the pro-regenerative potential of hAECs is associated with the gestational age of the fetus. We saw an initial early expansion of BASCs at D7 in animals given term hAECs, and this expansion was self-limiting by D14 (Figure 1). Similarly, term hAECs triggered a self-limiting expansion of AT2 cells at D5 which returned to quiescence by D14 (Figure 2). This suggests that any influence that term hAECs may have on the BASC and AT2 population is transient. This bodes well for future clinical applications where one may be concerned that progenitor cells could become constitutively activated and predisposed to tumorigenesis. And while Wnt/β-catenin signaling has been implicated in lung injury and repair, we did not observe any changes to β-catenin nuclear localization between groups (Figure 3).

In the present study, we observed reduction in transcriptional levels of *BMP4, RARRES2, SFRP2* and *TGFβ2* in total RNA from lungs of mice 14 days following bleomycin challenge (Figure 4). These were not restored to normal levels by administration of either term or preterm hAECs. However, bleomycin-related reduction in *BMP4* transcription was partially mitigated by term and preterm hAECs such that transcriptional levels were not significantly different from controls. These findings suggest that hAECs may support BASC proliferation through the reported BMP4–nuclear factor of activated T cells c1 (NFATc1)–thrombospondin-1 (TSP1) axis [20].

We observed that only the term hAECs were able to mitigate bleomycin-induced suppression of *WIF1* and *TGIF1* (Figure 4). The significant increase in *WIF1*, *TGIF* and *MYC* transcription at 14 days post-bleomycin challenge in mice given term hAECs, coincides with the return of BASCs to levels of quiescence— suggesting that *WIF1* and *TGIF* may also regulate the quiescence and self-renewal of BASCs. Wnt inhibitor factor 1 (*WIF1*) binds to Wnt proteins and sequesters them to the extracellular space, thereby inhibiting their binding to a receptor [30]. While *TGIF* inhibits the TGFβ signaling pathway by associating with *Smad2* and recruiting co-repressors, and is able to regulate quiescence and self-renewal of haematopoietic stem cells [31]. Since there was no difference in *MYC* transcriptional levels between term and preterm hAECs, the difference in *MYC* levels in hAEC treated mice was likely a reflection of endogenous *MYC*, which plays a critical role in maintaining the self-renewal capacity of BASCs [32].

When we assessed the expression of Wnt target genes in BASC and AT2 organoids, we observed significant changes in gene expression only in alveolar organoids from both AT2 and BASC origins that were co-cultured with term hAECs. Here we found that term hAECs were better able to influence these Wnt target genes involved in alveolar epithelium regeneration. They enhanced the expression of *BMP4* and *CDC42* in BASC induced alveolar organoids, and the expression of cell cycle related gene *CCND1* in both AT2 and BASC induced alveolar organoids. A previous report showed that *BMP4* induced lung endothelial cell activation directs BASC differentiation to the alveolar lineage through BMP4–NFATc1–TSP1 axis *in vivo* [20]. Cell division control protein 42 (*CDC42*) is an activator of the Fzd promoter, plays a vital role in lung epithelial cell proliferation, and is essential for formation and maintenance of the respiratory tract [33]. Interestingly, *FZD9* expression was down-regulated in both term and preterm hAEC co-cultures. Frizzled-9 (*FZD)9* acts as a tumor suppressor through the non-canonical Wnt pathway when bound to *WNT7A* [34]. Restoration of *WNT7A* and *FZD9* have been shown to inhibit the growth of murine lung carcinoma cells and human non-small cell lung cancer cells [35]. Down-regulation of *FZD9* in lung organoids may reflect the pro-proliferative effect of hAECs on the BASC and AT2 organoids. Furthermore, the differences in gene transcription

PORTLAND PRESS

of Wnt ligands between term and preterm hAECs may be partly due to corticosteroid exposure, commonly administered when preterm delivery is imminent and thus warrants further investigation.

The majority of miRNA content were similar between term and preterm donors. When commonly expressed miRNAs were assessed, we noted that 101 miRNAs were $\geq 2$-folds more abundant in term hAECs. Three of the 22 miRNAs (miR-302d, miR-1260b, miR-1291) that were expressed at 4-folds higher levels in term hAECs compared with preterm hAECs were associated with 34 genes of the Wnt signaling pathway. Two of the 19 miRNAs (miR-302d, miR-1260b, miR-1291) that were expressed 2-fold lower in term hAECs compared with preterm hAECs were associated with 27 genes of the Wnt signaling pathway. Five of the down-regulated miRNAs in term hAECs associated with 55 genes related to the Hippo signaling pathway, which regulates lung epithelial progenitor cell emergence and differentiation [36]. Interestingly, *YAP1,* which is crucial in regulating lung embryonic and adult stem cell differentiation [37], was increased in animals treated with term hAECs.

Taken together, our study suggests that the gestational age and possibly the pregnancy related complications that resulted in the premature delivery, of hAECs and potentially other perinatal stem and stem-like cells, can impact their regenerative potential. Differences in the ability of hAECs from term and preterm donors to activate lung stem cell niches, resulted in observable differences in their ability to enhance proliferation of resident stem/progenitor cells, and consequently augment their regenerative potential. It is important to note that this increase in endogenous stem/progenitor cell activity was transient, and reflective of the previous reports on the transient presence of hAECs following cell administration. The present study provides a better understanding of the mechanisms by which hAECs exert their regenerative actions, as well as indications to potency tests that should be implemented prior to clinical use of hAECs and other modalities of cell therapy. The present study also suggests that complications of pregnancy may impact quality of perinatal stem cells and thus necessitates further research as the banking of these perinatal stem cells become increasingly commonplace.

## Clinical perspectives

- Information around the impact of donor gestational age on the potency of the isolated perinatal cells remains scarce. We previously showed that human amniotic epithelial cells (hAECs) from term healthy pregnancy but not preterm pregnancy improves lung architecture in bleomycin-induced mouse lung injury. Here, we sought to understand the impact of donor gestational age on hAECs and their ability to activate endogenous lung stem/progenitor cells.

- We observed that term hAECs were better able to activate bronchioalveolar stem cells (BASCs) and type 2 alveolar epithelial cells (AT2s) compared with preterm hAECs in the context of bleomycin-induced lung injury.

- Our study suggests that the impact of gestational age on hAECs and potentially other perinatal stem and stem-like cells should be considered in clinical translation.

## Author Contribution

D.Z., R.S., S.T.C., J.T., M.S. and R.L. performed research, collected and analysed data presented in this manuscript. D.Z., M.S. G.D.K., R.S. and R.L. wrote the manuscript. K.T.L., C.K., E.M.W. and R.L. conceived and designed the research.

## Abbreviations

AT2, type 2 alveolar epithelial cell; BASC, bronchioalveolar stem cell; FZD9, Frizzled-9; hAEC, human amniotic epithelial cell; IPF, idiopathic pulmonary fibrosis; NFATc1, nuclear factor of activated T cells c1; TSP1, thrombospondin-1; WIF1, Wnt inhibitor factor 1.

## References

1 Lederer, D.J. and Martinez, F.J. (2018) Idiopathic Pulmonary Fibrosis. *N. Engl. J. Med.* **379**, 797–798

2 King, Jr, T.E., Pardo, A. and Selman, M. (2011) Idiopathic pulmonary fibrosis. *Lancet* **378**, 1949–1961, https://doi.org/10.1016/S0140-6736(11)60052-4

3 Molina-Molina, M. and Borie, R. (2018) Clinical implications of telomere dysfunction in lung fibrosis. *Curr. Opin. Pulm. Med.* **24**, 440–444, https://doi.org/10.1097/MCP.0000000000000506

4 Zhang, C., Yin, X., Zhang, J., Ao, Q., Gu, Y. and Liu, Y. (2017) Clinical observation of umbilical cord mesenchymal stem cell treatment of severe idiopathic pulmonary fibrosis: A case report. *Exp. Ther. Med.* **13**, 1922–1926, https://doi.org/10.3892/etm.2017.4222

5 Chambers, D.C., Enever, D., Ilic, N., Sparks, L., Whitelaw, K., Ayres, J. et al. (2014) A phase 1b study of placenta-derived mesenchymal stromal cells in patients with idiopathic pulmonary fibrosis. *Respirology* **19**, 1013–1018, https://doi.org/10.1111/resp.12343

6 Cargnoni, A., Gibelli, L., Tosini, A., Signoroni, P.B., Nassuato, C., Arienti, D. et al. (2009) Transplantation of allogeneic and xenogeneic placenta-derived cells reduces bleomycin-induced lung fibrosis. *Cell Transplant.* **18**, 405–422, https://doi.org/10.3727/096368909788809857

7 Barkauskas, C.E., Cronce, M.J., Rackley, C.R., Bowie, E.J., Keene, D.R., Stripp, B.R. et al. (2013) Type 2 alveolar cells are stem cells in adult lung. *J. Clin. Invest.* **123**, 3025–3036, https://doi.org/10.1172/JCI68782

8 Liu, Y., Kumar, V.S., Zhang, W., Rehman, J. and Malik, A.B. (2015) Activation of type II cells into regenerative stem cell antigen-1(+) cells during alveolar repair. *Am. J. Respir. Cell Mol. Biol.* **53**, 113–124, https://doi.org/10.1165/rcmb.2013-0497OC

9 Jain, R., Barkauskas, C.E., Takeda, N., Bowie, E.J., Aghajanian, H., Wang, Q. et al. (2015) Plasticity of Hopx(+) type I alveolar cells to regenerate type II cells in the lung. *Nat. Commun.* **6**, 6727, https://doi.org/10.1038/ncomms7727

10 Alder, J.K., Barkauskas, C.E., Limjunyawong, N., Stanley, S.E., Kembou, F., Tuder, R.M. et al. (2015) Telomere dysfunction causes alveolar stem cell failure. *Proc. Natl. Acad. Sci. U. S. A.* **112**, 5099–5104, https://doi.org/10.1073/pnas.1504780112

11 Kim, C.F., Jackson, E.L., Woolfenden, A.E., Lawrence, S., Babar, I., Vogel, S. et al. (2005) Identification of bronchioalveolar stem cells in normal lung and lung cancer. *Cell* **121**, 823–835, https://doi.org/10.1016/j.cell.2005.03.032

12 Tropea, K.A., Leder, E., Aslam, M., Lau, A.N., Raiser, D.M., Lee, J.H. et al. (2012) Bronchioalveolar stem cells increase after mesenchymal stromal cell treatment in a mouse model of bronchopulmonary dysplasia. *Am. J. Physiol. Lung Cell. Mol. Physiol.* **302**, L829–L837, https://doi.org/10.1152/ajplung.00347.2011

13 Tan, J.L., Lau, S.N., Leaw, B., Nguyen, H.P.T., Salamonsen, L.A., Saad, M.I. et al. (2018) Amnion Epithelial Cell-Derived Exosomes Restrict Lung Injury and Enhance Endogenous Lung Repair. *Stem Cells Transl. Med.* **7**, 180–196, https://doi.org/10.1002/sctm.17-0185

14 Lim, R., Malhotra, A., Tan, J., Chan, S.T., Lau, S., Zhu, D. et al. (2018) First-In-Human Administration of Allogeneic Amnion Cells in Premature Infants With Bronchopulmonary Dysplasia: A Safety Study. *Stem Cells Transl. Med.* **7**, 628–635, https://doi.org/10.1002/sctm.18-0079

15 Phan, T.G., Ma, H., Lim, R., Sobey, C.G. and Wallace, E.M. (2018) Phase 1 Trial of Amnion Cell Therapy for Ischemic Stroke. *Front. Neurol.* **9**, 198, https://doi.org/10.3389/fneur.2018.00198

16 Lim, R., Hodge, A., Moore, G., Wallace, E.M. and Sievert, W. (2017) A Pilot Study Evaluating the Safety of Intravenously Administered Human Amnion Epithelial Cells for the Treatment of Hepatic Fibrosis. *Front. Pharmacol.* **8**, 549, https://doi.org/10.3389/fphar.2017.00549

17 Lim, R., Chan, S.T., Tan, J.L., Mockler, J.C., Murphy, S.V. and Wallace, E.M. (2013) Preterm human amnion epithelial cells have limited reparative potential. *Placenta* **34**, 486–492, https://doi.org/10.1016/j.placenta.2013.03.010

18 Murphy, S., Rosli, S., Acharya, R., Mathias, L., Lim, R., Wallace, E. et al. (2010) Amnion epithelial cell isolation and characterization for clinical use. *Curr. Protoc. Stem Cell Biol.*, Chapter 1:Unit 1E 6, https://doi.org/10.1002/9780470151808.sc01e06s13

19 Murphy, S.V., Kidyoor, A., Reid, T., Atala, A., Wallace, E.M. and Lim, R. (2014) Isolation, cryopreservation and culture of human amnion epithelial cells for clinical applications. *J. Vis. Exp.* **94**, e52085, https://doi.org/10.3791/52085

20 Lee, J.H., Bhang, D.H., Beede, A., Huang, T.L., Stripp, B.R., Bloch, K.D. et al. (2014) Lung stem cell differentiation in mice directed by endothelial cells via a BMP4-NFATc1-thrombospondin-1 axis. *Cell* **156**, 440–455, https://doi.org/10.1016/j.cell.2013.12.039

21 Zhu, D., Tan, J., Maleken, A.S., Muljadi, R., Chan, S.T., Lau, S.N. et al. (2017) Human amnion cells reverse acute and chronic pulmonary damage in experimental neonatal lung injury. *Stem Cell Res. Ther.* **8**, 257, https://doi.org/10.1186/s13287-017-0689-9

22 Vosdoganes, P., Lim, R., Koulaeva, E., Chan, S.T., Acharya, R., Moss, T.J. et al. (2013) Human amnion epithelial cells modulate hyperoxia-induced neonatal lung injury in mice. *Cytotherapy* **15**, 1021–1029, https://doi.org/10.1016/j.jcyt.2013.03.004

23 Vosdoganes, P., Hodges, R.J., Lim, R., Westover, A.J., Acharya, R.Y., Wallace, E.M. et al. (2011) Human amnion epithelial cells as a treatment for inflammation-induced fetal lung injury in sheep. *Am. J. Obstet. Gynecol.* **205**, 156e26–156e33, https://doi.org/10.1016/j.ajog.2011.03.054

24 Liu, Q., Liu, K., Cui, G., Huang, X., Yao, S., Guo, W. et al. (2019) Lung regeneration by multipotent stem cells residing at the bronchioalveolar-duct junction. *Nat. Genet.* **51**, 728–738, https://doi.org/10.1038/s41588-019-0346-6

25 Murphy, S., Lim, R., Dickinson, H., Acharya, R., Rosli, S., Jenkin, G. et al. (2011) Human amnion epithelial cells prevent bleomycin-induced lung injury and preserve lung function. *Cell Transplant.* **20**, 909–923, https://doi.org/10.3727/096368910X543385

26 Moodley, Y., Ilancheran, S., Samuel, C., Vaghjiani, V., Atienza, D., Williams, E.D. et al. (2010) Human amnion epithelial cell transplantation abrogates lung fibrosis and augments repair. *Am. J. Respir. Crit. Care Med.* **182**, 643–651, https://doi.org/10.1164/rccm.201001-0014OC

27  Clevers, H., Loh, K.M. and Nusse, R. (2014) Stem cell signaling. An integral program for tissue renewal and regeneration: Wnt signaling and stem cell control. *Science* **346**, 1248012, https://doi.org/10.1126/science.1248012

28  Salwig, I., Spitznagel, B., Vazquez-Armendariz, A.I., Khalooghi, K., Guenther, S., Herold, S. et al. (2019) Bronchioalveolar stem cells are a main source for regeneration of distal lung epithelia in vivo. *EMBO J.* **38**, https://doi.org/10.15252/embj.2019102099

29  Kotton, D.N. and Morrisey, E.E. (2014) Lung regeneration: mechanisms, applications and emerging stem cell populations. *Nat. Med.* **20**, 822–832, https://doi.org/10.1038/nm.3642

30  Kawano, Y. and Kypta, R. (2003) Secreted antagonists of the Wnt signalling pathway. *J. Cell Sci.* **116**, 2627–2634, https://doi.org/10.1242/jcs.00623

31  Yan, L., Womack, B., Wotton, D., Guo, Y., Shyr, Y., Dave, U. et al. (2013) Tgif1 regulates quiescence and self-renewal of hematopoietic stem cells. *Mol. Cell. Biol.* **33**, 4824–4833, https://doi.org/10.1128/MCB.01076-13

32  Dong, J., Sutor, S., Jiang, G., Cao, Y., Asmann, Y.W. and Wigle, D.A. (2011) c-Myc regulates self-renewal in bronchoalveolar stem cells. *PLoS ONE* **6**, e23707, https://doi.org/10.1371/journal.pone.0023707

33  Wan, H., Liu, C., Wert, S.E., Xu, W., Liao, Y., Zheng, Y. et al. (2013) CDC42 is required for structural patterning of the lung during development. *Dev. Biol.* **374**, 46–57, https://doi.org/10.1016/j.ydbio.2012.11.030

34  Bikkavilli, R.K., Avasarala, S., Van Scoyk, M., Arcaroli, J., Brzezinski, C., Zhang, W. et al. (2015) Wnt7a is a novel inducer of beta-catenin-independent tumor-suppressive cellular senescence in lung cancer. *Oncogene* **34**, 5406, https://doi.org/10.1038/onc.2015.165

35  Winn, R.A., Van Scoyk, M., Hammond, M., Rodriguez, K., Crossno, Jr, J.T., Heasley, L.E. et al. (2006) Antitumorigenic effect of Wnt 7a and Fzd 9 in non-small cell lung cancer cells is mediated through ERK-5-dependent activation of peroxisome proliferator-activated receptor gamma. *J. Biol. Chem.* **281**, 26943–26950, https://doi.org/10.1074/jbc.M604145200

36  Mahoney, J.E., Mori, M., Szymaniak, A.D., Varelas, X. and Cardoso, W.V. (2014) The hippo pathway effector Yap controls patterning and differentiation of airway epithelial progenitors. *Dev. Cell* **30**, 137–150, https://doi.org/10.1016/j.devcel.2014.06.003

37  Lange, A.W., Sridharan, A., Xu, Y., Stripp, B.R., Perl, A.K. and Whitsett, J.A. (2015) Hippo/Yap signaling controls epithelial progenitor cell proliferation and differentiation in the embryonic and adult lung. *J. Mol. Cell Biol.* **7**, 35–47, https://doi.org/10.1093/jmcb/mju046

**Supplementary Table 1: Targeted genes and their assay ID in TaqMan assays:**

| Human TaqMan Assays | |
|---|---|
| **Gene name** | **TaqMan assay ID** |
| WNT1 | Hs01011247_m1 |
| WNT2 | Hs00608224_m1 |
| WNT2B | Hs00921614_m1 |
| WNT3 | Hs00902257_m1 |
| WNT3A | Hs00263977_m1 |
| WNT4 | Hs01573504_m1 |
| WNT5A | Hs00998537_m1 |
| WNT5B | Hs01086864_m1 |
| WNT6 | Hs00362452_m1 |
| WNT7A | Hs00171699_m1 |
| WNT7B | Hs00536497_m1 |
| WNT8A | Hs00230534_m1 |
| WNT8B | Hs00610126_m1 |
| WNT9A | Hs00243321_m1 |
| WNT9B | Hs00287409_m1 |
| WNT10A | Hs00228741_m1 |
| WNT10B | Hs00559664_m1 |
| WNT11 | Hs00182986_m1 |
| WNT16 | Hs00365138_m1 |
| MYC | Hs00153408_m1 |
| GAPDH | Hs02758991_g1 |

| Mouse TaqMan Assays | |
|---|---|
| **Gene name** | **TaqMan assay ID** |
| APC | Mm00545872_m1 |
| AXIN1 | Mm01299060_m1 |
| AXIN2 | Mm00443610_m1 |
| β-Catenin | Mm00458117_m1 |
| BMP4 | Mm00432087_m1 |
| BRCA1 | Mm00515386_m1 |
| CCND1 | Mm00432359_m1 |
| CCND2 | Mm00438070_m1 |
| CCND3 | Mm01612362_m1 |
| CDC42 | Mm01194005_g1 |
| CDK4 | Mm00726334_s1 |
| CSNK1G2 | Mm00506098_m1 |
| DKK1 | Mm00438422_m1 |
| DKK2 | Mm01322146_m1 |
| DKK4 | Mm00461141_m1 |
| DVL1 | Mm00438592_m1 |

| | |
|---|---|
| DVL2 | Mm00432899_m1 |
| DVL3 | Mm00432914_m1 |
| EFNB2 | Mm00438670_m1 |
| Elf2s3y | Mm01210630_m1 |
| FGF1 | Mm00438906_m1 |
| FGF2 | Mm00433287_m1 |
| FGF4 | Mm00438917_m1 |
| FGF7 | Mm00433291_m1 |
| FGF8 | Mm00438922_m1 |
| FGF9 | Mm00442795_m1 |
| FGFR1 | Mm00438930_m1 |
| FGFR2 | Mm01269930_m1 |
| FGFR3 | Mm00433294_m1 |
| FGFR4 | Mm01341852_m1 |
| FOXA2 | Mm01976556_s1 |
| FRZB (SFRP3) | Mm00441378_m1 |
| FZD1 | Mm00445405_s1 |
| FZD2 | Mm02524776_m1 |
| FZD3 | Mm00445423_m1 |
| FZD4 | Mm00433382_m1 |
| FZD5 | Mm00445623_s1 |
| FZD6 | Mm00433387_m1 |
| FZD7 | Mm00433409_m1 |
| FZD8 | Mm01234717_s1 |
| FZD9 | Mm01206511_s1 |
| FZD10 | Mm00558396_s1 |
| GATA6 | Mm00802636_m1 |
| GRB2 | Mm03023989_g1 |
| GSK3β | Mm00444911_m1 |
| IL1A | Mm00439620_m1 |
| IL1B | Mm00434228_m1 |
| IL6 | Mm00446190_m1 |
| KCNMA1 | Mm01268569_m1 |
| KDR | Mm01222421_m1 |
| KREMEN1 | Mm00459616_m1 |
| KREMEN2 | Mm01309205_m1 |
| HGF | Mm01135193_m1 |
| LEF1 | Mm00550265_m1 |
| LRP5 | Mm01227476_m1 |
| LRP6 | Mm00999795_m1 |
| MYCBP | Mm01192721_m1 |
| MYCL | Mm03053598_s1 |
| MYCN | Mm00476449_m1 |

| | |
|---|---|
| MST1R | Mm00436382_m1 |
| NMI | Mm00803857_m1 |
| PAK3 | Mm01332263_m1 |
| PECAM1 | Mm01242576_m1 |
| PLCG1 | Mm01247293_m1 |
| PLK3C2G | Mm00440781_m1 |
| RARA | Mm01296312_m1 |
| RARB | Mm01319677_m1 |
| RARRES1 | Mm01220691_m1 |
| RARRES2 | Mm00503579_m1 |
| RLF | Mm01181427_m1 |
| RSPO1 | Mm00507077_m1 |
| RXRB | Mm00441193_m1 |
| SFRP1 | Mm00489161_m1 |
| SFRP2 | Mm01213947_m1 |
| SFRP4 | Mm00840104_m1 |
| SFRP5 | Mm01194236_m1 |
| SOSTDC1(WISE) | Mm03024258_s1 |
| SRC | Mm00436785_m1 |
| TCF7 | Mm00493445_m1 |
| TCF7L1 | Mm01188711_m1 |
| TCF7l2 | Mm00501505_m1 |
| TGFA | Mm00446232_m1 |
| TGFB1 | Mm00441724_m1 |
| TGFB2 | Mm00436955_m1 |
| TGFB3 | Mm00436960_m1 |
| TGIF1 | Mm01227699_m1 |
| THBS1 | Mm00449032_g1 |
| TNF | Mm00443258_m1 |
| VEGFA | Mm00437304_m1 |
| WASF2 | Mm00463191_m1 |
| WIF1 | Mm00442355_m1 |
| YAP1 | Mm01143263_m1 |
| ID2 | Mm00711781_m1 |
| BIRC5 | Mm00599749_m1 |
| CTGF | Mm01192933_g1 |
| SMAD7 | Mm00484742_m1 |
| SMAD2 | Mm00487530_m1 |
| SMAD3 | Mm01170760_m1 |
| SMAD4 | Mm03023996_m1 |
| LATS1 | Mm01191886_m1 |
| LATS2 | Mm01321138_m1 |
| GAPDH | Mm03302249_g1 |

**Supplementary Table 2: miRNAs expressed at 2-flod or higher in term hAECs compared to preterm hAECs**

| Gene name | Fold change (Term Vs Preterm hAECs) |
|---|---|
| hsa-let-7f | 73.9252724 |
| hsa-miR-624 | 11.9606178 |
| hsa-miR-501-5p | 11.5893119 |
| hsa-miR-1267 | 9.40703942 |
| hsa-miR-10a | 9.33998835 |
| hsa-miR-30a-5p | 9.23908353 |
| hsa-miR-769-3p | 6.09007502 |
| hsa-miR-765 | 5.9368267 |
| hsa-miR-616 | 5.93591322 |
| hsa-miR-622 | 5.80398986 |
| hsa-miR-614 | 5.75760573 |
| hsa-miR-936 | 5.72195043 |
| hsa-miR-302d | 4.83553578 |
| hsa-miR-335 | 4.73486978 |
| hsa-miR-1260 | 4.67596701 |
| hsa-miR-320B | 4.64558651 |
| hsa-miR-1290 | 4.63298416 |
| hsa-miR-100 | 4.58483479 |
| hsa-miR-1291 | 4.5791212 |
| hsa-miR-135b | 4.56791799 |
| hsa-miR-205 | 4.56299398 |
| hsa-miR-146b-5p | 4.52565544 |
| hsa-miR-654-5p | 3.10642021 |
| hsa-miR-345 | 3.03995507 |
| hsa-miR-362-3p | 3.01261017 |
| hsa-miR-34a | 3.01110705 |
| hsa-miR-590-3P | 2.98324197 |
| hsa-miR-604 | 2.97292486 |
| hsa-miR-496 | 2.96894013 |
| hsa-miR-500 | 2.96631334 |
| hsa-miR-515-3p | 2.96351426 |
| hsa-miR-483-5p | 2.96316713 |
| hsa-miR-638 | 2.96307676 |
| hsa-miR-491-5p | 2.96063779 |
| hsa-miR-886-5p | 2.95575768 |
| hsa-miR-548E | 2.95336568 |
| hsa-miR-653 | 2.95306682 |
| hsa-miR-886-3p | 2.95226863 |
| hsa-miR-580 | 2.94765361 |
| hsa-miR-875-5p | 2.94732264 |

| | |
|---|---|
| hsa-miR-548L | 2.94185471 |
| hsa-miR-652 | 2.93768967 |
| hsa-miR-520g | 2.9331686 |
| hsa-miR-942 | 2.93215018 |
| hsa-miR-572 | 2.93123168 |
| hsa-miR-603 | 2.93006161 |
| hsa-miR-601 | 2.92240879 |
| hsa-miR-483-3p | 2.91913716 |
| hsa-miR-550 | 2.91420628 |
| hsa-miR-660 | 2.91405276 |
| hsa-miR-532-3p | 2.91197102 |
| hsa-miR-564 | 2.89349069 |
| hsa-miR-9 | 2.88646754 |
| hsa-miR-625 | 2.86010874 |
| hsa-miR-429 | 2.85665141 |
| hsa-miR-1244 | 2.4558335 |
| hsa-miR-1274B | 2.45036175 |
| hsa-miR-24 | 2.41474149 |
| hsa-miR-126 | 2.40232568 |
| hsa-miR-1248 | 2.39443579 |
| hsa-miR-21 | 2.39229574 |
| hsa-miR-27b | 2.38572168 |
| hsa-miR-125b | 2.38510826 |
| hsa-miR-200a | 2.38357455 |
| hsa-miR-339-3p | 2.36985986 |
| hsa-miR-16 | 2.36078678 |
| hsa-miR-190b | 2.35740682 |
| hsa-miR-182 | 2.35422425 |
| hsa-miR-1282 | 2.34712512 |
| hsa-miR-183 | 2.34537522 |
| hsa-miR-29a | 2.34277881 |
| hsa-miR-148b | 2.33849404 |
| hsa-miR-302a | 2.3347608 |
| hsa-miR-210 | 2.33292956 |
| hsa-miR-136 | 2.33038569 |
| hsa-miR-15a | 2.31586435 |
| hsa-miR-26a | 2.31559789 |
| hsa-let-7a | 2.3138683 |
| hsa-miR-24-2 | 2.31292863 |
| hsa-miR-135b | 2.31255512 |
| hsa-miR-184 | 2.3124926 |
| hsa-miR-151-3p | 2.31168328 |
| hsa-miR-1303 | 2.30981251 |

| | |
|---|---|
| hsa-miR-125a-5p | 2.30917378 |
| hsa-miR-30d | 2.30753055 |
| hsa-miR-33a | 2.30252808 |
| hsa-miR-21 | 2.29932237 |
| hsa-miR-1285 | 2.29742498 |
| hsa-miR-126 | 2.29467963 |
| hsa-miR-1243 | 2.29330581 |
| hsa-miR-203 | 2.29226645 |
| hsa-let-7b | 2.29098935 |
| hsa-miR-152 | 2.28618595 |
| hsa-miR-23a | 2.27398344 |
| hsa-miR-193b | 2.26861493 |
| hsa-miR-148b | 2.24852161 |
| hsa-miR-206 | 2.24723773 |
| hsa-miR-338-5P | 2.15202934 |
| hsa-miR-193a-5p | 2.0961773 |

**Supplementary Table 3: Pathways union of 22 most upregulated miRNAs in term hAECs compared to preterm hAECs**

| KEGG pathway | p-value | #genes | #miRNAs |
|---|---|---|---|
| Hippo signaling pathway | 1.87e-10 | 97 | 11 |
| Proteoglycans in cancer | 2.22e-16 | 128 | 10 |
| Lysine degradation | 3.22e-10 | 27 | 8 |
| Adherens junction | 2.43e-09 | 49 | 8 |
| Glioma | 1.2e-10 | 42 | 7 |
| Transcriptional misregulation in cancer | 2.92e-06 | 68 | 7 |
| Colorectal cancer | 4.26e-07 | 42 | 5 |
| Central carbon metabolism in cancer | 0.000551468 | 35 | 5 |
| Oocyte meiosis | 0.01050969 | 52 | 5 |
| Fatty acid biosynthesis | 0 | 4 | 4 |
| Pathways in cancer | 0 | 170 | 4 |
| Fatty acid metabolism | 2.46e-14 | 12 | 4 |
| ECM-receptor interaction | 2.25e-07 | 41 | 4 |
| Viral carcinogenesis | 1.69e-05 | 76 | 4 |
| Pancreatic cancer | 3.84e-05 | 39 | 4 |
| Cell cycle | 0.001057385 | 56 | 4 |
| p53 signaling pathway | 0.008877096 | 31 | 4 |
| TGF-beta signaling pathway | 0.009077201 | 23 | 4 |
| Bladder cancer | 0.0303866 | 27 | 4 |
| Chronic myeloid leukemia | 8.52e-07 | 36 | 3 |
| Steroid biosynthesis | 1.08e-06 | 13 | 3 |
| MicroRNAs in cancer | 2.61e-05 | 31 | 3 |
| Signaling pathways regulating pluripotency of stem cells | 0.000101375 | 56 | 3 |
| Hepatitis B | 0.000116071 | 65 | 3 |
| Non-small cell lung cancer | 0.00106916 | 19 | 3 |
| Wnt signaling pathway | 0.001600731 | 34 | 3 |
| Mucin type O-Glycan biosynthesis | 0.01146427 | 15 | 3 |
| Prostate cancer | 0.01627984 | 41 | 3 |
| Endometrial cancer | 0.01806197 | 24 | 3 |
| Protein processing in endoplasmic reticulum | 0.03844125 | 64 | 3 |

| | | | |
|---|---|---|---|
| Melanoma | 0.05479326 | 29 | 3 |
| Thyroid hormone signaling pathway | 0.07510067 | 43 | 3 |
| MAPK signaling pathway | 0.2362782 | 55 | 3 |
| Thyroid cancer | 0.2421421 | 17 | 3 |
| RNA transport | 0.2476021 | 47 | 3 |
| Arrhythmogenic right ventricular cardiomyopathy (ARVC) | 0.2902186 | 14 | 3 |
| Epstein-Barr virus infection | 0.8280952 | 69 | 3 |
| Small cell lung cancer | 0.001958015 | 39 | 2 |
| ErbB signaling pathway | 0.2967561 | 20 | 2 |
| HIF-1 signaling pathway | 0.4232772 | 20 | 2 |
| Estrogen signaling pathway | 0.5800298 | 15 | 2 |
| Prolactin signaling pathway | 0.7940552 | 12 | 2 |
| Base excision repair | 0.9166133 | 9 | 2 |
| Ribosome | 0.9359495 | 27 | 2 |
| Circadian rhythm | 0.9375584 | 12 | 2 |
| PI3K-Akt signaling pathway | 0.9446857 | 81 | 2 |
| Endocytosis | 0.955366 | 42 | 2 |
| Parkinson's disease | 0.965306 | 11 | 2 |
| Pyrimidine metabolism | 0.9999214 | 11 | 2 |
| Acute myeloid leukemia | 0.02043816 | 16 | 1 |
| Renal cell carcinoma | 0.03886262 | 13 | 1 |
| FoxO signaling pathway | 0.2141295 | 32 | 1 |
| HTLV-I infection | 0.2418832 | 21 | 1 |
| Ubiquitin mediated proteolysis | 0.2485583 | 42 | 1 |
| Biotin metabolism | 0.6066103 | 1 | 1 |
| Basal cell carcinoma | 0.7988809 | 15 | 1 |
| Ras signaling pathway | 0.8403023 | 20 | 1 |
| Bacterial invasion of epithelial cells | 0.8754792 | 15 | 1 |
| Focal adhesion | 0.9008744 | 18 | 1 |
| Spliceosome | 0.9298831 | 14 | 1 |
| TNF signaling pathway | 0.9391868 | 10 | 1 |
| Shigellosis | 0.9656469 | 7 | 1 |
| Leukocyte transendothelial migration | 0.9689753 | 5 | 1 |
| Apoptosis | 0.9782784 | 17 | 1 |

| | | | |
|---|---|---|---|
| Toxoplasmosis | 0.9879972 | 13 | 1 |
| Neurotrophin signaling pathway | 0.9880193 | 12 | 1 |
| mTOR signaling pathway | 0.9896191 | 8 | 1 |
| mRNA surveillance pathway | 0.9918225 | 23 | 1 |
| Nucleotide excision repair | 0.9934617 | 8 | 1 |
| Sphingolipid signaling pathway | 0.9941056 | 11 | 1 |
| VEGF signaling pathway | 0.9951137 | 9 | 1 |
| Gap junction | 0.9965675 | 1 | 1 |
| NF-kappa B signaling pathway | 0.9973862 | 7 | 1 |
| Melanogenesis | 0.9987607 | 13 | 1 |
| Glycosphingolipid biosynthesis - lacto and neolacto series | 0.9989954 | 2 | 1 |
| Cytokine-cytokine receptor interaction | 0.9995343 | 61 | 1 |
| Choline metabolism in cancer | 0.9995538 | 11 | 1 |
| Chagas disease (American trypanosomiasis) | 0.9998149 | 11 | 1 |
| Proteasome | 0.9998363 | 6 | 1 |
| Valine, leucine and isoleucine biosynthesis | 0.9999118 | 1 | 1 |
| Huntington's disease | 0.9999144 | 28 | 1 |
| Fc epsilon RI signaling pathway | 0.9999492 | 11 | 1 |
| Oxidative phosphorylation | 0.9999511 | 11 | 1 |
| D-Glutamine and D-glutamate metabolism | 0.9999547 | 1 | 1 |
| Thyroid hormone synthesis | 0.9999614 | 11 | 1 |
| Cell adhesion molecules (CAMs) | 0.9999652 | 29 | 1 |
| 2-Oxocarboxylic acid metabolism | 0.9999719 | 2 | 1 |
| Carbon metabolism | 0.9999867 | 9 | 1 |
| Amoebiasis | 0.9999911 | 11 | 1 |
| DNA replication | 0.9999984 | 5 | 1 |
| Biosynthesis of amino acids | 0.9999985 | 8 | 1 |
| One carbon pool by folate | 0.9999993 | 1 | 1 |
| Purine metabolism | 0.9999996 | 15 | 1 |
| Other types of O-glycan biosynthesis | 0.9999998 | 2 | 1 |
| Toll-like receptor signaling pathway | 0.9999999 | 10 | 1 |
| Primary bile acid biosynthesis | 1 | 6 | 1 |

| | | | |
|---|---|---|---|
| Sulfur metabolism | 1 | 2 | 1 |
| Homologous recombination | 1 | 4 | 1 |
| Salivary secretion | 1 | 27 | 1 |

**Supplementary Table 4: miRNAs expressed at 2-fold decrease or lower in term hAECs compared to preterm hAECs**

| Gene name | Fold change (Term Vs Preterm hAECs) |
|---|---|
| hsa-miR-520c-3p | 0.004527985 |
| hsa-miR-519b-3p | 0.018013443 |
| hsa-miR-520h | 0.03558593 |
| hsa-miR-520D-3P | 0.035845622 |
| hsa-miR-10b | 0.140716436 |
| hsa-miR-145 | 0.270838877 |
| hsa-miR-668 | 0.2731444 |
| hsa-miR-454 | 0.284359666 |
| hsa-miR-409-3p | 0.286356399 |
| hsa-miR-29b-1 | 0.28661137 |
| hsa-miR-770-5p | 0.287529871 |
| hsa-miR-34b | 0.287689555 |
| hsa-miR-27a | 0.28903032 |
| hsa-miR-370 | 0.356659671 |
| hsa-miR-520e | 0.359573349 |
| hsa-miR-200b | 0.361049863 |
| hsa-miR-127-3p | 0.362306602 |
| hsa-miR-487b | 0.364577643 |
| hsa-miR-25 | 0.365880137 |

**Supplementary Table 5: Pathways union of 2-flod decrease or lower expressed miRNAs in term hAECs compared to preterm hAECs**

| KEGG pathway | p-value | #genes | #miRNAs |
|---|---|---|---|
| Pathways in cancer | 7.09736e-09 | 123 | 5 |
| Adherens junction | 7.230013e-09 | 34 | 5 |
| Viral carcinogenesis | 2.314077e-08 | 58 | 5 |
| Hippo signaling pathway | 9.020322e-06 | 55 | 5 |
| Chronic myeloid leukemia | 0.01043694 | 34 | 5 |
| Fatty acid metabolism | 3.321574e-05 | 10 | 4 |
| Lysine degradation | 0.0001861324 | 15 | 4 |
| Glioma | 0.0007934242 | 26 | 4 |
| TGF-beta signaling pathway | 0.00299193 | 30 | 4 |
| p53 signaling pathway | 0.0153499 | 30 | 4 |
| Prostate cancer | 0.04877802 | 37 | 4 |
| Bacterial invasion of epithelial cells | 0.07623696 | 36 | 4 |
| Thyroid hormone signaling pathway | 0.08919184 | 37 | 4 |
| FoxO signaling pathway | 0.1396272 | 45 | 4 |
| MicroRNAs in cancer | 0 | 47 | 3 |
| Fatty acid elongation | 2.221477e-05 | 3 | 3 |
| Signaling pathways regulating pluripotency of stem cells | 8.977921e-05 | 42 | 3 |
| Focal adhesion | 0.0009282172 | 66 | 3 |
| Colorectal cancer | 0.001894819 | 27 | 3 |
| Transcriptional misregulation in cancer | 0.003153647 | 31 | 3 |
| Endometrial cancer | 0.009056928 | 20 | 3 |
| Hepatitis B | 0.009636186 | 35 | 3 |
| PI3K-Akt signaling pathway | 0.1100134 | 89 | 3 |
| Central carbon metabolism in cancer | 0.2034327 | 18 | 3 |
| Cell cycle | 0.8333105 | 34 | 3 |
| Fatty acid biosynthesis | 0 | 2 | 2 |
| Bladder cancer | 0.008888864 | 14 | 2 |
| Fatty acid degradation | 0.1516373 | 6 | 2 |
| Melanoma | 0.1939439 | 16 | 2 |
| Small cell lung cancer | 0.2118684 | 29 | 2 |
| Amoebiasis | 0.252933 | 27 | 2 |

| | | | |
|---|---|---|---|
| Wnt signaling pathway | 0.3382355 | 27 | 2 |
| Protein processing in endoplasmic reticulum | 0.5435447 | 18 | 2 |
| Non-small cell lung cancer | 0.5459003 | 15 | 2 |
| Pancreatic cancer | 0.6407905 | 20 | 2 |
| Renal cell carcinoma | 0.800708 | 18 | 2 |
| ErbB signaling pathway | 0.8720876 | 22 | 2 |
| Axon guidance | 0.9803328 | 20 | 2 |
| Endocytosis | 0.1280316 | 21 | 1 |
| Ubiquitin mediated proteolysis | 0.366851 | 23 | 1 |
| HTLV-I infection | 0.6535317 | 36 | 1 |
| Arrhythmogenic right ventricular cardiomyopathy (ARVC) | 0.7019688 | 12 | 1 |
| Thyroid cancer | 0.8192068 | 4 | 1 |
| Cell adhesion molecules (CAMs) | 0.8207323 | 1 | 1 |
| HIF-1 signaling pathway | 0.8268555 | 12 | 1 |
| N-Glycan biosynthesis | 0.8416644 | 1 | 1 |
| Prolactin signaling pathway | 0.8454987 | 15 | 1 |
| Oocyte meiosis | 0.8486408 | 17 | 1 |
| AMPK signaling pathway | 0.9244279 | 3 | 1 |
| Neurotrophin signaling pathway | 0.9315332 | 14 | 1 |
| Glycosaminoglycan degradation | 0.9651712 | 3 | 1 |
| Rap1 signaling pathway | 0.9888523 | 1 | 1 |
| Pathogenic Escherichia coli infection | 0.9919459 | 7 | 1 |
| Inflammatory bowel disease (IBD) | 0.9962719 | 7 | 1 |
| Dorso-ventral axis formation | 0.9977154 | 6 | 1 |
| Ras signaling pathway | 0.9978458 | 23 | 1 |
| Glycosaminoglycan biosynthesis - chondroitin sulfate / dermatan sulfate | 0.9984241 | 1 | 1 |
| Huntington's disease | 0.9991098 | 7 | 1 |
| Steroid biosynthesis | 0.9992379 | 3 | 1 |
| Mucin type O-Glycan biosynthesis | 0.9995166 | 1 | 1 |
| Dilated cardiomyopathy | 0.9999237 | 13 | 1 |
| Fc gamma R-mediated phagocytosis | 0.999948 | 11 | 1 |
| Pyrimidine metabolism | 0.9999537 | 7 | 1 |
| Other glycan degradation | 0.9999543 | 1 | 1 |

| | | | |
|---|---|---|---|
| Inositol phosphate metabolism | 0.9999657 | 1 | 1 |
| Hypertrophic cardiomyopathy (HCM) | 0.9999665 | 12 | 1 |
| Valine, leucine and isoleucine degradation | 0.9999786 | 5 | 1 |
| Leukocyte transendothelial migration | 0.9999984 | 13 | 1 |
| Other types of O-glycan biosynthesis | 0.9999994 | 2 | 1 |
| Glycosphingolipid biosynthesis - lacto and neolacto series | 0.9999998 | 2 | 1 |
| Sulfur metabolism | 1 | 2 | 1 |